Bose-Hubbard Model

Stanimir Kondov

May 5, 2008

Abstract

The Bose-Hubbard hamiltonian will be introduced and justified as an effective description of some relevant physical systems (dilute alkali gases in optical lattices, arrays of Josephson junctions). I will also show a mean field theory solution and the resulting phase diagram. Finally, I will describe in detail one of the more important experiments with an optical lattice of ^{87}Rb atoms.

1. The Bose-Hubbard Hamiltonian

The Bose-Hubbard hamiltonian is an effective hamiltonian that resides on a lattice ([1], [2]). It is given by

$$H = -\omega \sum_{<i,j>} (b_i^\dagger b_j + b_j^\dagger b_i) - \mu \sum_i n_i + U \sum_i n_i(n_i - 1), \tag{1}$$

where

$$\begin{aligned} \left[b_i, b_j^\dagger\right] &= \delta_{ij} \\ n_i &= b_i^\dagger b_i \end{aligned} \tag{2}$$

are respectively the boson field operators and the boson number operator. The commutation relation of these operators ensures the correct symmetrization properties for the Fock eigenspace occupied by the system of bosons.

Now examine the hamiltonian term by term. The angular brackets in the first sum restrict the summation over nearest neighbors only. The first term can be interpreted as the exchange energy for bosons at neighboring sites, and is also known as the hopping or tunneling term. An explicit integral expression for the tunneling matrix element could look like

$$\omega = -\int d^3x w(x - x_i) \left(\frac{-\hbar^2 \nabla^2}{2m} + V(x) \right) w(x - x_j). \tag{3}$$

w here is the single-site Wannier function, the concept of which comes up in the familiar tight binding model.

The second term in (1) accounts for the chemical potential, which fixes the particle number in the grand canonical ensemble. The third term is a way to put in a repulsive ($U > 0$) or attractive interaction among bosons on the same lattice point.

2. **Mean Field Solution and Phase Diagram**

In a simple mean-field theoretical approach, we introduce the complex parameter ψ, and the hamiltonian

$$H_{MF} = \sum_i \left(-\mu n_i + U n_i(n_i - 1) - \psi^\star b_i - \psi b_i\right). \tag{4}$$

This is basically an on-site hamiltonian, where the influence from neighboring sites has been replaced by a complex variational parameter. We are free to vary ψ to minimize the ground state energy, and the variational argument tells us that this minimum will not underestimate the exact value.

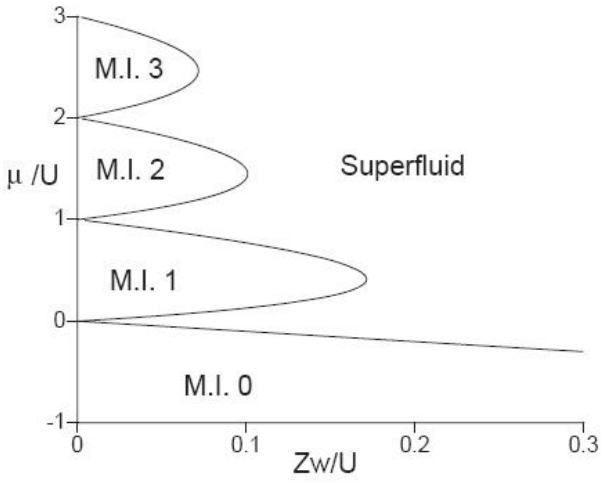

Figure 1: Phase diagram as predicted by mean field theory.

Let us explore a couple of limiting cases in order to obtain some understanding for the phase diagram (Fig.1). When interactions dominate the Hamiltonian ($\omega = 0$) the mean field theory is exact, and $\psi = 0$. The on-site particle number states are the eigenstates of the hamiltonian, and the energy E is given by

$$E = -\mu M + UM(M-1) = UM^2 - (\mu + U)M, \tag{5}$$

where M is the on-site particle number. The value of M that minimizes the energy is $M = 1 + \mu/U$. Note however that we have to round off to the nearest

whole number (n_0). This implies a degeneracy for the values $\mu/U \in \mathbf{N}$, which will be lifted when we allow for $\omega > 0$.
Now allow for small ω in the hamiltonian. The tunneling term can be treated as a perturbation, which is shown below to commute with the rest of the hamiltonian.

$$\begin{aligned}\left[n_i, \sum_{<ij>}\left(b_i^\dagger b_j + b_j^\dagger b_i\right)\right] &= \sum_{<ij>}\left(b_i^\dagger b_i b_i^\dagger b_j + b_i^\dagger b_i b_j^\dagger b_i - b_i^\dagger b_j b_i^\dagger b_i - b_j^\dagger b_i b_i^\dagger b_i\right) = \\ &= \sum_{<ij>}\left(b_i^\dagger b_j - b_j^\dagger b_i\right) = \\ &= 0 \end{aligned} \tag{6}$$

In the last line the sum is taken over all nearest neighbors, and all terms get canceled by antisymmetry.
The fact that the perturbation commutes with the rest of the hamiltonian tells us that if we increase ω adiabatically, the system will evolve in an eigenstate of $N = \sum_i n_i$ with precisely the same eigenvalue. Thus, for a small but finite ω, we obtain the exact result:

$$\langle n_i \rangle = n_0(\mu/U) \tag{7}$$

The above argument explains the existence of the islands of fixed particle number in the phase diagram. Those islands are referred to as the Mott Insulator (M.I.) phase. This phase is known as incompressible, since

$$\frac{\partial \langle N \rangle}{\partial \mu} = 0. \tag{8}$$

The value of an observable is fixed at a quantized value over a finite part of the phase diagram. This is a typical signature of quantum phase transitions, which will be expanded upon in the next section. Again, this phenomenon is only made possible by the existence of a perturbation that commutes with the hamiltonian.
In the opposite limit we take the tunneling to dominate the hamiltonian ($\omega \gg |U|$). The ground state will consist of particle states that are delocalized over the whole lattice. Neighboring sites will be strongly coupled and ψ will assume a non-zero value. We can take the difference between the true ground state energy and the mean field ground state energy (ΔE) and we can minimize it with respect to ψ to obtain

$$\begin{aligned}\frac{\Delta E}{M} &= -z\omega \left\langle b^\dagger \right\rangle \langle b \rangle + \langle b \rangle \psi^\star + \left\langle b^\dagger \right\rangle \psi \\ \Rightarrow \psi &= z\omega \langle b \rangle . \end{aligned} \tag{9}$$

When tunneling dominates the hamiltonian the ground state is no longer an eigenstate of the number operator, but rather

$$|\Psi\rangle_{\omega \gg |U|} \propto \left(\sum_i a_i^\dagger \right)^N |0\rangle \,. \tag{10}$$

ψ will then acquire a finite value, and the system will be in the superfluid (S.F.) state.

Some explanation is due here as to why we dubbed the two phases Mott insulator and superfluid. It is clear by now that the field ψ is a good candidate for an order parameter. Therefore the phase transition is well-defined. Superfluidity required long-range order, and ψ is itself a non-zero off-diagonal element (it is proportional to the expectation value of the boson annihilation operator). Furthermore, finite ψ breaks the $b \to be^{i\theta}$ symmetry present in (1), and provides a stiffness to variations in phase. This is another signature of ODLRO, and so we can rightfully call the phase superfluid.

Finally, let us use mean field theory to determine the phase boundary. This can be done using phenomenological Landau theory. We can define a Landau free energy of the form:

$$L = r|\psi|^2 + s|\psi|^4 + \mathcal{O}(|\psi|^6). \tag{11}$$

The phase transition will occur when $r = 0$, and that can be found using second order perturbation theory.

$$r = \xi(\mu/U) \left[1 - z\omega\xi(\mu/U) \right], \tag{12}$$

where

$$\xi(\mu/U) = \frac{n_0(\mu/U) + 1}{Un_0(\mu/U) - \mu} + \frac{n_0(\mu/U)}{\mu - U(n_0(\mu/U) - 1)}. \tag{13}$$

Solving this expression for $r = 0$ gives the phase boundaries of Fig.1.

3. The Quantum Phase Transition

Now that we have looked at the phase transition in descriptive detail, it may be worthwhile to reconsider our results in the broader light of quantum phase transitions. A quantum phase transition is a transition that is driven by quantum mechanical and not by thermal fluctuations. As a system approaches the absolute zero thermal fluctuations are frozen out, and quantum mechanical effects become more and more relevant. Therefore a system will be allowed to undergo a quantum phase transition even at zero Kelvin.

There is a caveat to the whole story just as in the case of classical phase transitions. A system with a finite number of degrees of freedom is described by a partition function that is a sum of a finite number of terms. Those terms are all analytic and therefore the partition function (and all derivatives) are also analytic. The explanation for non-analytic behavior we found in taking the limit of infinite system size (an infinite sum of analytic functions can give a non-analytic result).

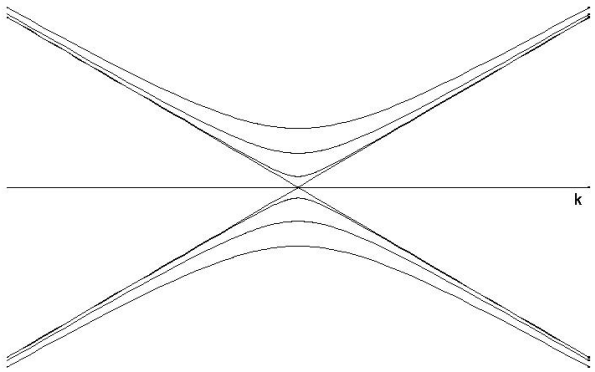

Figure 2: Avoided crossings (as a function of the parameter k) can become sharper and sharper with increasing particle number.

In the case of quantum phase transitions we will have to rely on the same argument but for a different reason. The energy states of a system are the eigenvalues of the hamiltonian which is a hermitian matrix whose entries depend on a small number of external parameters. Now, it can be shown mathematically that the eigenvalues of a hermitian matrix that depend on N continuous real parameters cannot cross except at a manifold of $N-2$ dimensions. So for a large system that depends on a few parameters the energy levels will avoid crossing. As long as we evolve parameters adiabatically, a system in the ground state will stay in the ground state. However, as we increase the system size, the avoided crossing will become sharper and sharper, so in the infinite system limit it will approach its asymptotic cone (Fig.2). The adiabatic theorem will then become irrelevant and a phase transition will be possible.

4. **Experimental Verification**

The analysis of the Bose-Hubbard hamiltonian has been helpful in explaining electron localization in Josephson junction arrays ([3]) and superfluid Helium in porous media. However, most of the interest nowadays lies in dilute alkali gases trapped in periodic optical potentials (optical lattices). In those experiments atoms are trapped and cooled to degeneracy in potentials of standing electromagnetic waves ([4]). Well-controlled potential depths and geometries have turned optical lattice experiments into dedicated quantum simulations for condensed-matter theories.

The first and most famous observation of the S.F. to M.I. transition ([5]) was

done using about $2 \cdot 10^5$ ^{87}Rb (bosonic) atoms in a potential of the form

$$V = V_0 \left[sin^2(kx) + sin^2(ky) + sin^2(kz) \right] \tag{14}$$

encompassed by a harmonic potential envelope (Fig.3).

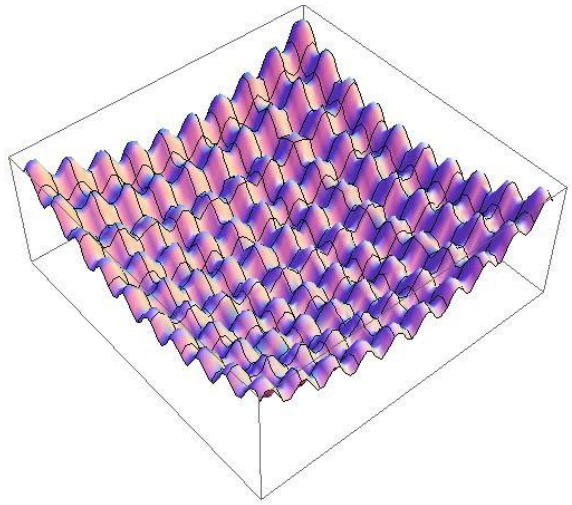

Figure 3: Sinusoid potential with harmonic envelope (here 2D only).

Periodic distance in this trap is chosen much larger than the inter-particle interaction distance. The number of atoms in the trap fixes the overall chemical potential, and the depth of the trap V_0 sets the ratio ω/U. Now that we are at a certain point on the phase diagram, we are free to adjust V_0 (laser intensity) across the critical point.

The measurement technique is nothing more than taking an absorbtion image of the atomic cloud immediately after the periodic potential is turned off. One atomic cloud thus gives a single data point. Any continuous curve of data will then involve the preparation of many atomic clouds.

So what do we expect to see for each phase? If the atoms are in the S.F. phase, then the ground state is delocalized across the lattice, and there is a high degree of phase coherence. Immediately when we release the atoms we expect to see a sharp interference pattern with the same symmetry as the initial trapping potential (simple cubic in this case). Note that this is actually matter-wave interference!

In the M.I. regime the atoms are strongly localized on separate sites. Number fluctuations are energetically very expensive and phase is not well-defined across the atomic cloud. When we release the trap we will see no interference peaks. Fig.4 shows false color pictures taken across the phase diagram. It seems like the interference peaks are gradually lost for smaller values of ω/U. However, the peak width does not increase. Instead, there is a stronger and

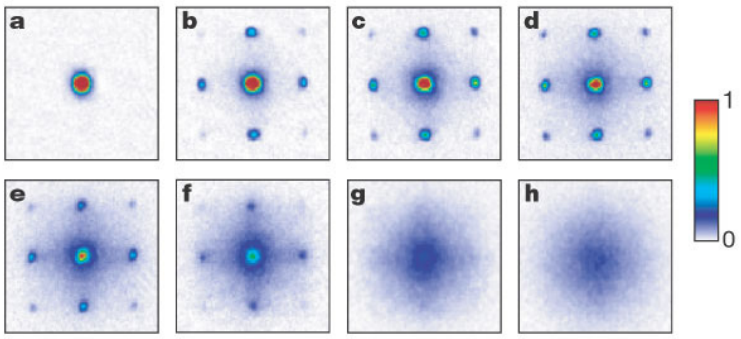

Figure 4: Absorption images taken after releasing the atoms from a periodic potential of increasing (a→h) depth.

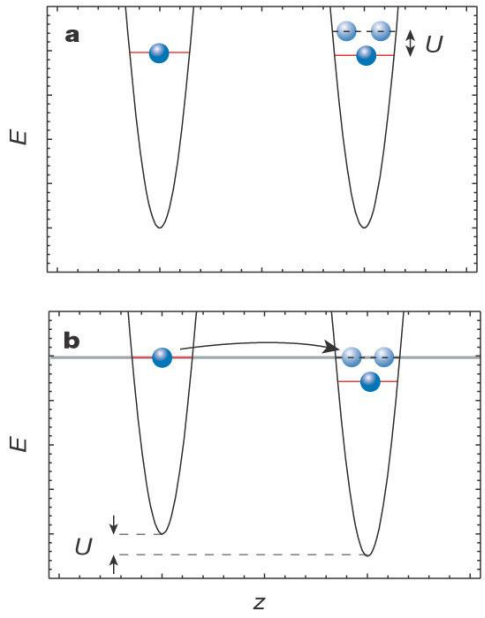

Figure 5: **(a)** The energy gap required to move a particle to an occupied lattice point. **(b)** A "leaning" perturbing potential makes tunneling energetically possible.

stronger background of M.I., which is controlled by the overall harmonic envelope of the magnetic trap. Strictly speaking, the atomic cloud is not a point, but rather a vertical line segment on the phase diagram.

Lastly, this paper introduces another measurement that unambiguously recognizes the M.I. phase. One property of the M.I. is that its excitation spectrum is gapped. It takes a finite amount of energy to create a particle-hole excitation, which in a simple cartoon picture (Fig.5a) can be thought of as the energy U required to place a particle in the neighboring site, where there is already

a particle present. So if we have to put two particles in the same potential well, we have to "lean" the lattice by introducing the right amount of potential gradient (Fig.5b).

The state preparation is described in Fig.6a. The graph shows the potential depth V_0 as a function of time. At first the periodic field is turned on adiabatically slow to ensure that the system evolves in the ground state ($\Delta\tau = 80ms$). When it reaches the maximum (V_{max}) value, we turn on a perturbing "leaning" field ($20ms$). Again, only the right amount of leaning will create a particle-hole excitation. Next, we relax the periodic potential to values that would correspond to the S.F. phase. If we had the right amount of "leaning" then, we will end up in an excited state of the system. The excitations are fluctuations in the phase which will result in broadening of the diffraction peaks (Fig.5b).

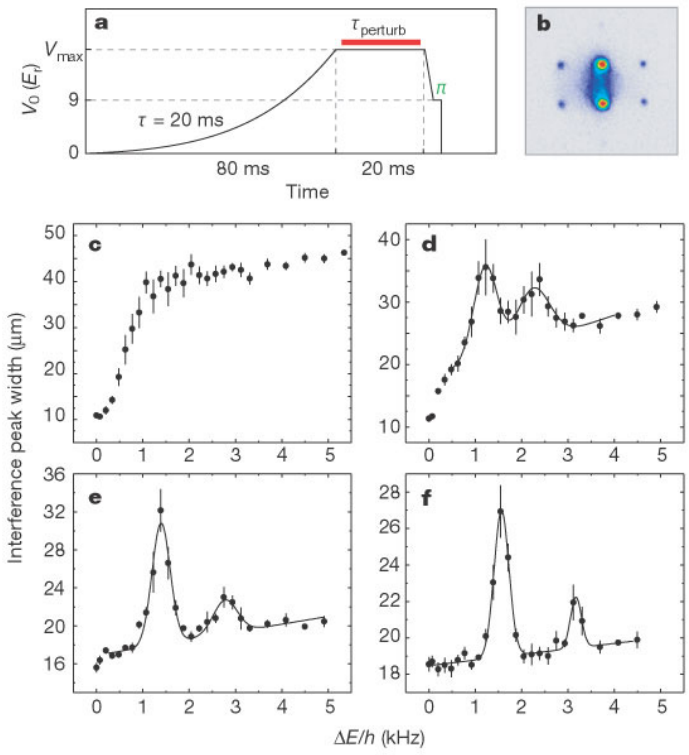

Figure 6: **(a)** Time sequence of optical lattice depth V_0 in preparation of the system in an excited state. **(b)** Peak broadening in S.F. interference due to excited state initialization. **(c)-(f)** Peak broadening data reveals the gapped excitation spectrum of M.I. phase. Consecutive graphs taken for larger values of V_0.

Fig.5c shows interference peak width as a function of potential gradient. The spikes at $\Delta E/h = 1.4$ and $\Delta E/h = 2.8$ show the quantized energy of the excitation gap. Peak broadening becomes more obvious for larger V_{max}, which corresponds to larger fraction of the cloud prepared in the excited M.I. state.

5. Conclusion

By far we have introduced the Bose-Hubbard hamiltonian, and we have looked at the different terms, giving them physical meaning. Several limiting cases have been introduced to help us visualize the phase diagram, and an analytic expression has been introduced to describe the exact phase boundary (within the mean field theory approximation). Then we considered the M.I.-S.F. transition in the broader light of quantum phase transitions, in which kinetic and potential energy compete to determine different ground states for the system. Finally, we overviewed a central experimental result that reveals some of the expected signatures of the M.I. and the S.F. phases.

A further direction of interest would be to allow for disorder in the model and consider the various (and sometimes contradicting) theoretical predictions, as well as to explore experimental observations thereof. Sadly, we must defer this to a later and more extensive study of this topic.

6. References

[1] M. P. A. Fisher, P. B. Weichman, G. Grinstein, and D. S. Fisher, Phys. Rev. B 40, 546 (1989), Boson localization and the superfluid-insulator transition

[2] Sachdev S., Quantum phase transitions

[3] One-dimensional Mott localization of quantum vortices in Josephson-junction arrays, A. van Oudenaarden, B. van Leeuwen, M. P. M. Robbens, and J. E. Mooij, PRL 57

[4] H. Metcalf, P. v. d. Straten, Laser cooling and trapping

[5] Quantum phase transition from a superfluid to a Mott insulator in a gas of ultracold atoms, M Greiner, O Mandel, TW Hänsch, I Bloch, Nature 415